

# UC Irvine

## UC Irvine Previously Published Works

### Title

Finite Element Analysis of Soccer Ball-Related Ocular and Retinal Trauma and Comparison with Abusive Head Trauma

### Permalink

<https://escholarship.org/uc/item/0d32m1x3>

### Journal

Ophthalmology Science, 2(2)

### ISSN

2666-9145

### Authors

Lam, Matthew R  
Dong, Pengfei  
Shokrollahi, Yasin  
et al.

### Publication Date

2022-06-01

### DOI

10.1016/j.xops.2022.100129

Peer reviewed



# Finite Element Analysis of Soccer Ball-Related Ocular and Retinal Trauma and Comparison with Abusive Head Trauma

Matthew R. Lam, BA,<sup>1</sup> Pengfei Dong, PhD,<sup>2</sup> Yasin Shokrollahi, MS,<sup>2</sup> Linxia Gu, PhD,<sup>2</sup>  
Donny W. Suh, MD, FAAP<sup>3</sup>

**Purpose:** Trauma to the eye resulting from a soccer ball is a common sports-related injury. Although the types of ocular pathologic features that result from impact have been documented, the underlying pathophysiologic mechanics are not as well studied. The purpose of this study was to evaluate the biomechanical events after the collision of a soccer ball with the eye to better understand the pathophysiology of observed ocular and retinal injuries and to compare them with those observed in abusive head trauma (AHT).

**Design:** Computer simulation study.

**Participants:** None.

**Methods:** A finite element model of the eye was used to investigate the effects of a collision of a soccer ball on the eye.

**Main Outcome Measures:** Intraocular pressure and stress.

**Results:** Impact of the soccer ball with the eye generated a pressure wave that traveled through the vitreous, creating transient pockets of high and negative pressure. During the high-frequency phase, pressure in the vitreous near the posterior pole ranged from 39.6 to -30.9 kPa. Stress in ocular tissue was greatest near the point of contact, with a peak of 66.6 kPa. The retina experienced the greatest stress at the vasculature, especially at distal branches, where stress rose to 15.4 kPa. On average, retinal stress was greatest in the subretinal layer, but was highest in the preretinal layer when considering only vascular tissue.

**Conclusions:** The high intraocular pressure and stress in ocular tissue near the point of soccer ball impact suggest that injuries to the anterior segment of the eye can be attributed to direct transmission of force from the ball. The subsequent propagation of a pressure wave may cause injuries to the posterior segment as the positive and negative pressures exert compressive and tractional forces on the retina. The linear movement of the pressure wave likely accounts for localization of retinal lesions to the posterior pole or superior temporal quadrant. The primarily linear force in soccer ball trauma is the probable cause for the more localized injury profile and lower retinal hemorrhage incidence compared with AHT, in which repetitive angular force is also at play. *Ophthalmology Science* 2022;2:100129 © 2022 by the American Academy of Ophthalmology. This is an open access article under the CC BY-NC-ND license (<http://creativecommons.org/licenses/by-nc-nd/4.0/>).

Sports-related injuries to the eye are common in the United States and across the globe, with as many as 600 000 injuries occurring each year in the United States alone, incurring a cost of more than \$300 000 000.<sup>1,2</sup> Injuries are seen most often in male teenage patients, with more than half of patients being  $\leq 18$  years of age and boys constituting  $> 80\%$  of patients seeking treatment at the emergency department.<sup>3,4</sup> Given that roughly 13 500 cases advance to blindness,<sup>5</sup> sports-related injuries result in approximately 759 000 life-years of vision loss annually in the United States.<sup>3,6</sup> Although basketball and baseball are the leading causes of sports-related injury to the eye in the United States, soccer is the most played game in the world and is the greatest source of sports-related eye injury in Europe and Israel.<sup>7,8</sup> In addition to its global prevalence, soccer is a sport of particular interest because it results in visual impairment at a disproportionately high rate.<sup>3</sup>

A variety of injuries can arise after collision of a rapidly moving soccer ball with the eye, including, but not limited to, corneal abrasion, hyphema, angle recession, retinal hemorrhage, and retinal detachment.<sup>7</sup> Rarely, injuries can advance to vision loss and even blindness, potentially leading to a dramatic reduction in quality of life and productivity by precipitating additional injuries, psychological stress leading to depression, significant financial burden, and other sequelae.<sup>3</sup>

Although pathologic features resulting from soccer ball ocular trauma (SBOT) have been documented, the underlying mechanics of the traumatic event that causes the various injuries observed have not yet been explored to the same degree. In this work, the authors present a computational basis for commonly presenting eye injuries using a finite element (FE) computer simulation of a soccer ball colliding with a human eye. In this type of simulation, a

human eye can be modeled by arranging building block-like elements that resemble bricks or plates (3-dimensional solid and 2-dimensional shell elements, respectively) into the various structures that compose the eye. Models are built using a large quantity of very small elements, allowing for granular spatial discretization of ocular structures. Attributes of these elements can be adjusted to mimic the mechanical properties of the corresponding tissues in a human eye. Interactions between elements can also be manipulated to achieve better anatomic accuracy, for example, by modeling the adhesions between the vitreous and retina. A soccer ball can then be modeled, allowing for a simulation of a collision with the eye using parameters representative of a typical kick. Finally, the simulation can visualize how the energy of the ball is transferred to the eye and how stress is distributed throughout the eye as influenced by the different mechanical properties of its various components. Through the simulated collision, it is possible to observe the pattern of stress distribution within the eye both spatially and temporally and to identify locations and time points of high stress. Investigation of these points allows for the development of a quantifiable basis for injuries to the eye that are commonly observed in SBOT. Establishing a quantitative understanding of SBOT will provide a foundation for further work such as comparing the efficacy of preventative measures and interventions like protective eyewear.

The FE simulation of the eye used in this investigation was also used by the authors in a previous work studying the deleterious effects of abusive head trauma (AHT) to the eyes of infants, most commonly associated with shaken baby syndrome.<sup>9</sup> Studying SBOT with the same model will allow for direct comparison of the 2 types of trauma and will provide insight into their different injury patterns. Providing a mechanical basis for these differences will assist in understanding symptomatic patterns of other ocular injuries as well as promoting a confident differential diagnosis of AHT, which is of great importance from not only a medical perspective, but a legal perspective as well.

## Methods

### Computational Simulation of Soccer Ball Impact

Transient dynamic analysis of the response of the eye to soccer ball impact in an FE simulation was performed using Abaqus/Explicit 2019 (Dassault Systèmes Simulia Corp). A streamlined FE eye model adopted from the authors' previous work studying AHT was used in the simulation.<sup>9</sup> This model was informed by a review of the literature to gather parameters and to ensure consensus with several other recently developed models of the eye. The streamlined model contained the sclera, vitreous, and retina, but excluded the cornea, iris, lens, and anterior segment to reduce confounding factors when investigating the effect of soccer ball impact on the retina. To approximate the dimensions of a healthy adult eye,<sup>10</sup> the sclera and retina were simulated as hollow spheres with outer diameters of 26 and 24.5 mm, respectively, and thicknesses of 0.8 and 0.25 mm, respectively. Furthermore, the retina was simulated as 3 thin layers to account for its preretinal, intraretinal, and subretinal layers. The vitreous was simulated as a filled sphere with a diameter of 24 mm.

Vitreoretinal attachments were incorporated along the retinal vessels, posterior pole, and vitreous base, where adhesions are strongest.<sup>11,12</sup> Finally, the eye was fixed at 4 points along the surface of the sclera, 7.8 mm from the center of the sclera and 90° from each other, and at the posterior pole (Fig 1B). These points represent the 4 extraocular rectus muscles and the optic nerve head, together providing the boundary condition. The material properties of the model are listed in Table 1.<sup>9</sup>

The soccer ball was simulated as a rigid sphere with a surface diameter of 220 mm that collided with the streamlined eye model with a velocity of 51 mph (22.8 m/s) and impact depth of 0.5 mm to emulate the conditions of a typical kick of a regulation-sized soccer ball.<sup>13</sup> In a soccer match, such a velocity can be reached in the setting of penalty kicks or free kicks, in which defenders are typically 10 to 11 m away. In free kicks in particular, defenders usually do not protect their faces and may even attempt to use their faces to stop the ball. The impact depth of the soccer ball was limited by the boundary condition to emulate the energy-dampening effect of the orbit. Velocity changes of the soccer ball and impact depth are difficult to determine through *in vivo* or *in vitro* experiments because of the complexity of an actual soccer ball impact with a human eye, in which the player's head and body also react to the collision. Therefore, these values were directly manipulated in this simulation to simplify the model and to study the response of the eye to an impact (Fig 1). The velocity of the ball during travel was assumed to be constant because the simulation time is relatively short. Deceleration of the ball likely would not be substantial enough to significantly reduce impact energy. Deceleration and rebound acceleration of the ball after collision were defined via stepwise velocity change, which was also unlikely to cause results to differ from *in vivo* observations given the short impact duration. The soccer ball was simulated as a solid body rather than a deformable body to focus on the mechanical events within the eye, rather than the interaction between a deforming ball and the orbit. These simplifications were not anticipated to significantly influence results.

The eye and soccer ball models were meshed with 140 770 and 10 096 elements for the computational simulation, respectively. This allowed for detailed analysis of interactions between the components of the eye at any of 140 770 locations. Stress in the retina at different layers and at locations of interest, as well as the pressure in the vitreous, were also examined. These measurements were made in terms of kilopascals, which are commonly used to describe biomechanical measurements of stress and pressure, allowing for direct comparison and clinical correlation.<sup>9,11,14–16</sup> Individual patient-level consent was not required for this study. All research adhered to the tenets of the Declaration of Helsinki.

## Results

The FE simulation revealed that direct collision of a soccer ball with the eye transiently deformed the globe by compressing it by 10% along the anterior–posterior axis and produced an indentation of 0.5 mm at the anterior pole (Fig 2). Impact of the ball initiated a shockwave in the vitreous that propagated posteriorly (Fig 2). On contact of the ball with the eye at  $t = 0.5$  ms, intraocular pressure in the vitreous closest to the point of impact at the anterior pole rose acutely to a peak value of 2.3 MPa. This localized pocket of high pressure then traveled linearly toward the posterior pole in the form of a dome-shaped compression pressure wave ( $t = 0.525–0.575$  ms). The vitreous pressure

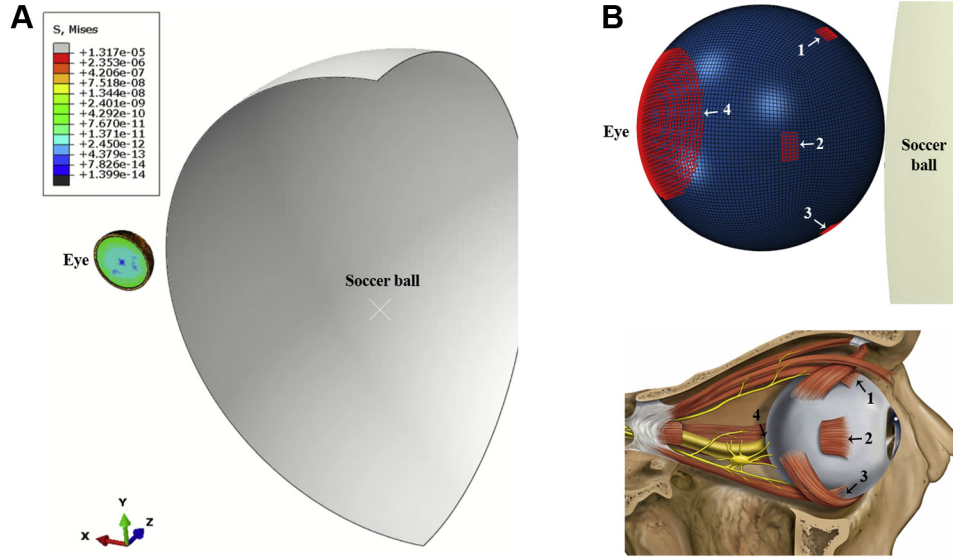


**Figure 1.** A, Simulation setup with the eye model (left) and soccer ball (cut view; right). B, Eye model showing boundary condition points highlighted in red (left). These boundary condition points represent the insertion points of the extraocular rectus muscles and the optic nerve head. The numerical labels correspond with the structures as follows: 1, superior rectus muscle; 2, medial or lateral rectus muscle; 3, inferior rectus muscle; and 4, optic nerve head. The medial or lateral rectus muscle on the opposite side of the eye was also simulated, but is not pictured. A reference diagram is provided below. (Adapted from Patrick J. Lynch, medical illustrator; C. Carl Jaffe, MD, cardiologist, CC BY 2.5).

was higher at the center of the compression pressure wave than the peripheral aspect of the wave, and the pressure in the wake of the pressure wave was negative. The pressure wave traveled from the anterior pole to the posterior pole in less than 0.1 ms. The peak value of the compression pressure declined to approximately 95 kPa during this propagation. The pressure wave then reflected from the retina ( $t = 0.6\text{--}0.625$  ms) and traveled between the 2 poles with high frequency for a couple of cycles. The subsequent pressure wave was of low frequency with positive pressure only. A history of pressures in the vitreous adjacent to the posterior pole and adjacent to the peripheral retina may be visualized in Figure 3. Vitreous near the posterior pole demonstrated greater positive and negative pressure fluctuations than vitreous near the periphery during the high-frequency stage, reaching 39.6 kPa and  $-30.9$  kPa compared with 24.8 kPa and  $-13.4$  kPa, respectively.

Load transmission in the ocular tissue was investigated as stress distribution at different time points after soccer ball impact (Fig 4). Stress was first experienced at the point of contact at the anterior pole with a peak stress value of

66.6 kPa, then was transmitted posteriorly through the ocular tissue. Four elements were selected from the peripheral retina to posterior retina to quantify this load transmission pattern, illustrated in Figure 4B as elements a through d (highlighted in Fig 4A). The posterior pole demonstrated increased stress earlier than the surrounding tissue at  $t = 0.6$  ms because of the pressure wave in the vitreous reaching the posterior pole. This is consistent with the observation that the pressure wave travels in an anterior to posterior direction in  $< 0.1$  ms. This can be observed in both Figure 4A at  $t = 0.6$  to  $0.7$  ms and in Figure 4B at  $t = 0.7$  ms, when element d, which represents the posterior pole, experienced higher stress than the rest of the selected elements except element a, which represents more anterior retinal tissue. However, on a longer time scale of 10 ms, the peripheral retina (element b) showed higher peak values of stress than the posterior pole (element d). Stress at posterior elements initially peaked at approximately  $t = 1$  ms, indicating that load transmission through the ocular tissue (approximately 0.5 ms) was slower than anterior–posterior pressure wave

Table 1. Material Properties of the Eye Components

Component	Material Model	Density (kg/m <sup>3</sup> )	Coefficients
Sclera	Mooney-Rivlin	1243	$\nu = 0.49$ , $A = 495$ , $B = -470.2$
Retina	Elastic	1000	$\nu = 0.49$ , $E = 11$ kPa
Vitreous	Viscoelastic	1009	$G_0 = 0.01$ kPa, $G_\infty = 3 \times 10^{-4}$ kPa, $B = 14.26$ s <sup>-1</sup> , $k = 2 \times 10^6$ kPa

A = Mooney-Rivlin constants; B = frequency; E = Young's modulus;  $G_0$  = instantaneous shear modulus;  $G_\infty$  = long-term shear modulus; k = Bulk modulus.

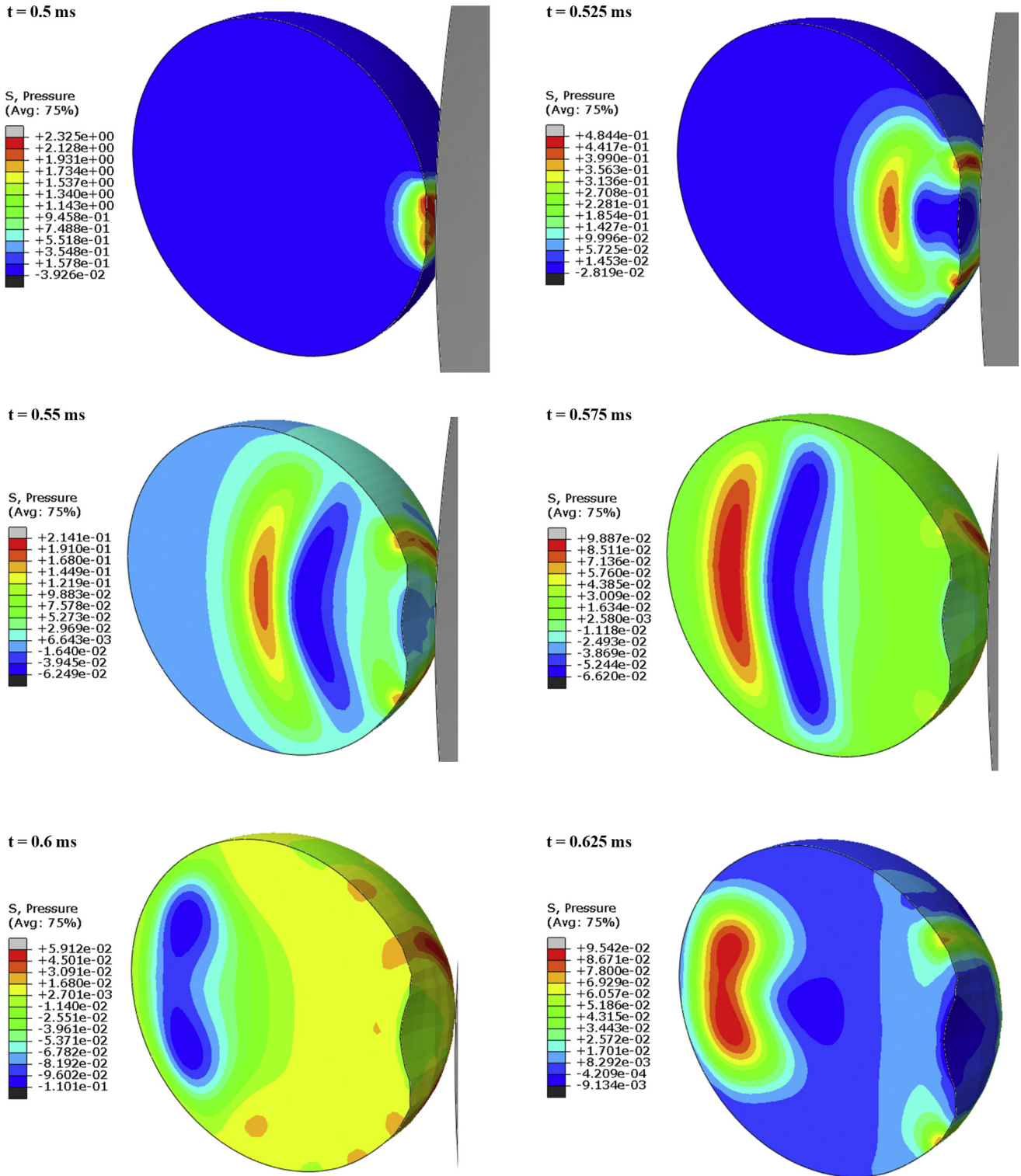


Figure 2. Distribution of pressure in the vitreous at different time points after impact of soccer ball (grey) at the anterior pole.

propagation through the vitreous (0.1 ms), likely because of the spherical structure and different wave speed through the tissue.

Ocular tissue 4 mm posterior to the anterior pole, where structures such as the iris and ciliary body are expected to be

found,<sup>17–20</sup> was studied at 3 adjacent elements. Stress initially reached values as high as 25.2 kPa, then fell to 5 to 10 kPa (Fig 5).

The force in the retina is depicted in Figures 6, 7, and 8 in terms of stress. The average stress in the retina was greater

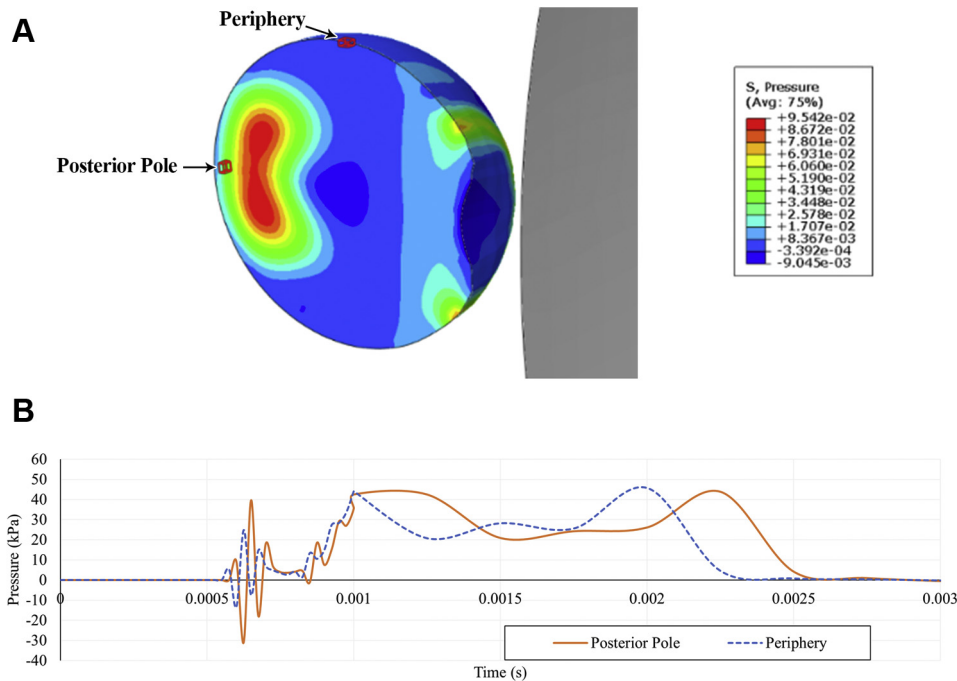


**Figure 3.** Pressure history in the vitreous adjacent to posterior pole and peripheral retina after impact of a soccer ball at the anterior pole. **A**, Diagram showing selected elements of interest in the vitreous near the posterior pole and peripheral retina, which are outlined in red on the eye (left). Gray object (right) represents the soccer ball. **B**, Line graph showing pressure history in the vitreous at the selected elements near the posterior pole and periphery.

along the vasculature compared with nonvascular tissue after initially peaking at similar values (Fig 6A). Distal vasculature branches and bifurcations experienced the highest stress, with a peak value of 15.4 kPa being observed among 6 representative elements at distal branches (Fig 7). The average stresses in the 3 component layers of the retina are shown in Figure 8. On average, the subretinal layer of the retina experienced more stress than the preretinal and intraretinal layers after impact, peaking near 7 kPa compared with roughly 3.5 kPa in the preretinal layer and 4.5 kPa in the intraretinal layer. When stress is calculated only at the vascular retinal tissue, the opposite trend is observed, with average stress highest in the preretinal layer and lowest in the subretinal layer.

## Discussion

### Anterior Segment

In a collision of a soccer ball with an eye, transmission of the kinetic energy propelling the ball to the eye causes compression of the globe and coerces it to temporarily adopt an ellipsoid shape. Structures near the point of impact may also be compressed as a result. This simulation provides a quantifiable basis for the observations of previous studies demonstrating that most soccer ball injuries involve the anterior portion of the eye.<sup>7</sup>

Hyphema is among the most commonly observed injuries after SBOT, being observed in as high as 50% of patients.<sup>7</sup> It is caused most frequently by blunt trauma,

especially sports-related injury, in which the impact of the blunt object briefly increases intraocular pressure and generates a direct force on the ciliary body and iris, tearing the blood vessels within.<sup>21,22</sup> The stress at the ciliary body may be sufficient to cause tearing between the longitudinal and circular muscles, resulting in angle recession seen in 71% to 100% of eyes with hyphema and frequently reported after SBOT.<sup>7,21,23,24</sup> These components of the eye lie roughly 3 to 5 mm posterior to the cornea in adults, where stress reached values as high as 25.2 kPa in the simulated globe (Fig 4). High stress on the ciliary body and iris can also likely account for the prevalence of uveitis in patients with soccer ball injury, because blunt trauma is a common cause of traumatic iritis.<sup>7,25</sup>

Glaucoma may arise secondary to blunt trauma, such as a soccer ball collision, resulting from various causes. Injury associated with angle recession and subsequent fibrosis in the trabecular meshwork and Schlemm's canal advances to secondary glaucoma in 7% to 9% of patients with angle recession, especially those with recession of 180° or more.<sup>23,24,26</sup> In addition, hyphema introduces cellular debris from macrophages and red blood cells into the anterior chamber that may impede drainage of aqueous humor and give rise to hemolytic glaucoma.<sup>27</sup> The depth of the anterior chamber in newborns is 1.5 to 2.9 mm, implying that younger patients may be at greater risk for the aforementioned pathologic features after SBOT because of a more anteriorly positioned ciliary body and iris.<sup>28</sup>

The peak vitreous pressure of 2.3 MPa (17 251.4 mmHg) recorded in this simulation exceeds the threshold for dynamic globe rupture of approximately 0.91 to 0.97 MPa

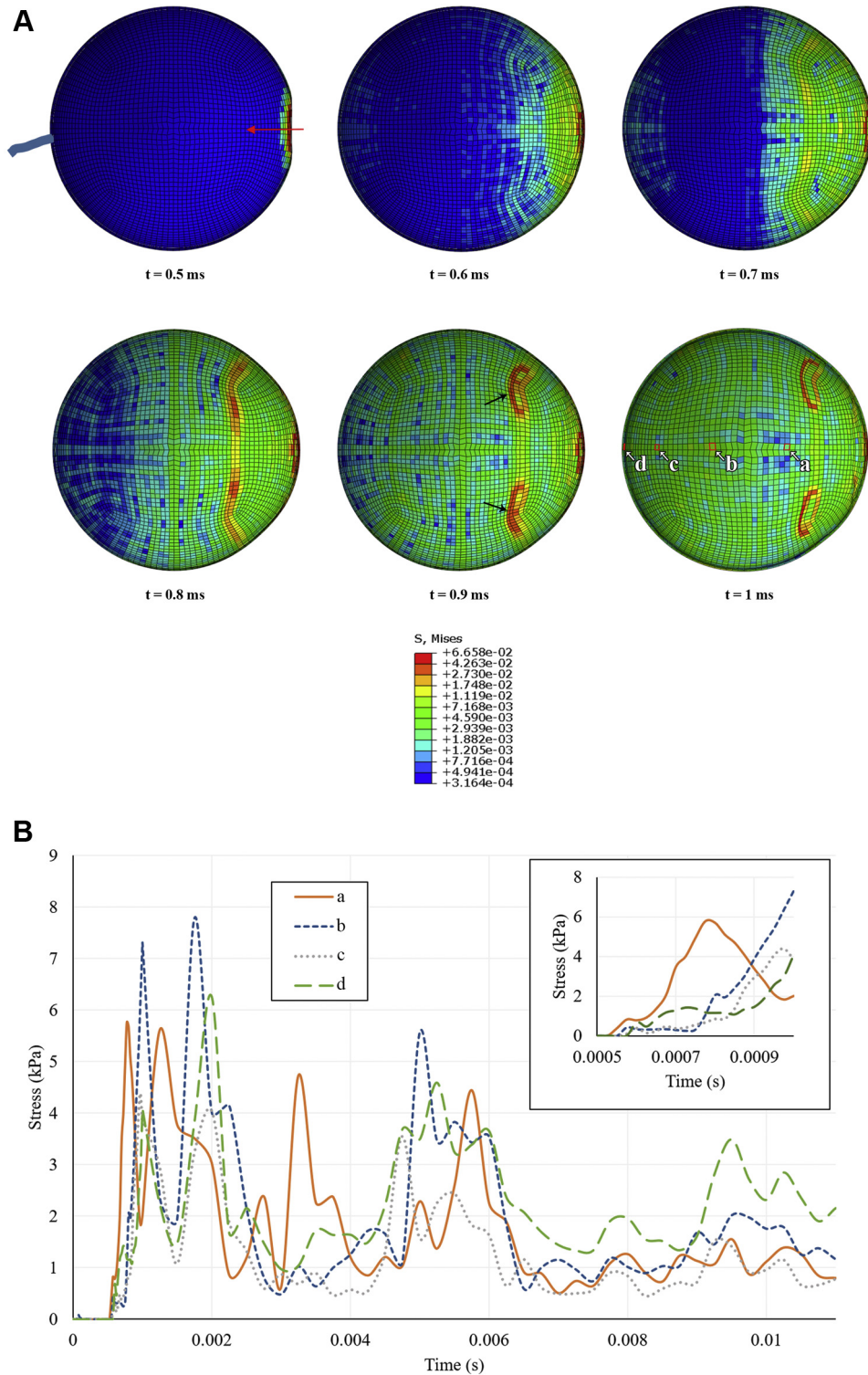


**Figure 4.** Stress distribution in ocular tissue at different time points after impact of a soccer ball at the anterior pole. **A,** Sagittal cross-section stress heatmaps of ocular tissue. For each heatmap, the anterior pole is on the right side of the image, denoted by the red arrow in the first time point. The 4 selected elements of interest (a–d), which represent progressively posterior ocular tissue, are outlined in red on the final time point. Circular regions of high stress in anterior ocular tissue that begin to emerge at  $t = 0.7$  ms and are most prominent at  $t = 0.9$  ms (black arrows) represent the attachment points of the extraocular rectus muscles. **B,** Line graph showing stress history in ocular tissue at selected elements along the anterior–posterior axis.

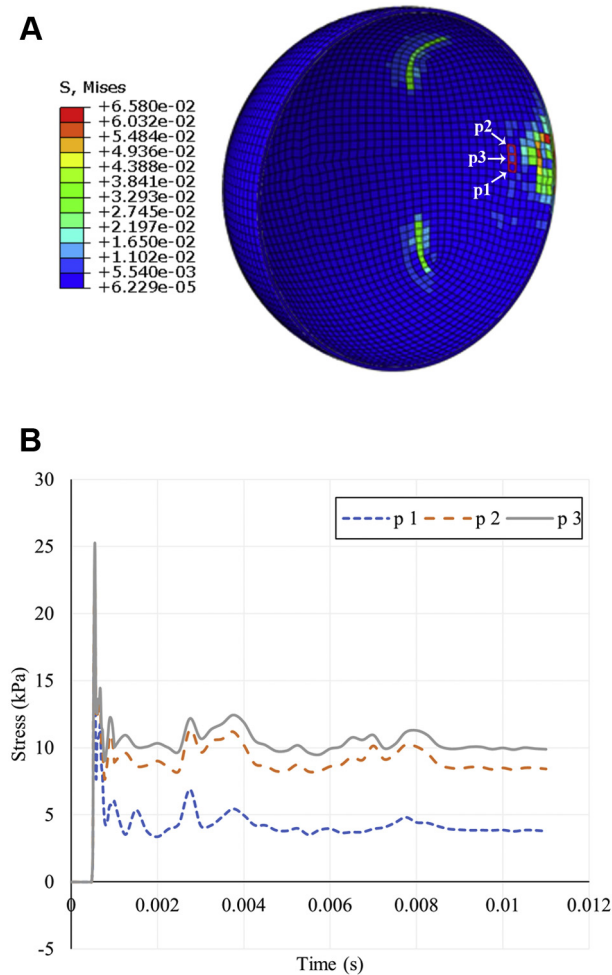


**Figure 5.** Stress distribution in the ocular tissue after impact of a soccer ball at the anterior pole, with emphasis on tissue located 4 mm posterior to the cornea, the approximate position of the ciliary body. **A**, Sagittal cross-section stress heatmap of ocular tissue. The anterior pole is on the right side of the image. The 3 selected elements of interest (p1, p2, and p3), which represent a sampling of ocular tissue near the position of the ciliary body, are outlined in red. **B**, Line graph showing stress history in ocular tissue at the selected 3 elements.

(6825.6–7275.6 mmHg),<sup>15,29,30</sup> yet few, if any, reports of globe rupture resulting from SBOT have been published.<sup>13</sup> This discrepancy can be reconciled by considering the localization of the pressure. Visualized in Figure 2 at  $t = 0.5$  ms, intraocular pressure reaches a peak value of 2.3 MPa only near the point of contact of the ball as energy is transferred from the ball to the eye. Because the high pressure is concentrated at the anterior segment and has not yet propagated throughout the vitreous, little to no excess pressure is exerted on most of the globe interior, making globe rupture unlikely. As energy disperses from the point of impact into the vitreous, intraocular pressure rises more uniformly, but at a lower peak value, as the energy dissipates. The vitreous pressure near the peripheral and posterior retina never exceeds 50 kPa, far below the threshold for globe rupture (Fig 3).

Injury to the anterior segment is influenced by the orbit, which provides protection to the eye through multiple mechanisms.<sup>31,32</sup> The bones of the orbit absorb much of the soccer ball's energy,<sup>13</sup> likely dampening the initial transfer of energy to the anterior segment of the globe and reducing subsequent transmission of force into the posterior segment. Additionally, the orbital walls allow only the small portion of the ball that deforms into the orbital opening on collision to contact the eye.<sup>13</sup> Lower orbital penetration of the soccer ball compared with other smaller sports balls may aid in preventing globe rupture by reducing excess compression of the globe. The degree of protection and consequent ocular damage may vary because of anatomic variations of the orbit, such as the depth at which the globe is recessed in relationship to the frontal orbit. For instance, the eyes of patients with thyroid-associated ophthalmopathy or other causes of proptosis are more exposed and benefit less from the protection conferred by the orbit. Although the orbit is not simulated in this current model, the boundary condition applied to the eye mimics the resistance of the orbit on the ball by controlling the impact depth of the ball. Limiting the contact of the ball with the eye with this restraint produces results similar to those that would be seen in the presence of the orbit. In future works, we aim to model the orbit and characterize the soccer ball as deformable, rather than rigid, to investigate if and how this interaction produces a different velocity profile. Although precise stress and pressure values and rates may vary slightly as a result, the overall trends elucidated by this current simplified model are likely to remain true.

Whether the eyelid also provides substantial protection to the eye during SBOT is unclear. A 2015 FE simulation by Liu et al<sup>33</sup> predicted that the energy absorbed by the eyelid during blunt trauma by a BB pellet would not be sufficient to reduce stress on the retina significantly, making it unlikely that the eyelid would reduce retinal stress induced by a soccer ball. The study also found that the eyelid protected the cornea by distributing force over a larger surface area, but the effect was less pronounced with pellets of larger diameter. This suggests that the effect would be minimal with a soccer ball, but epidemiologic data show that corneal abrasion occurs less frequently than hyphema or vitreous and retinal hemorrhage,<sup>7</sup> suggesting that the eyelids do protect the cornea to some degree if the person closes their eyes in time.

## Posterior Segment

The rapidly oscillating pressure within the vitreous suggests a possible mechanism for the posterior segment retinal lesions seen in SBOT.<sup>34,35</sup> The authors postulate that these pressure changes stress the intraocular tissues as alternating instances of high and negative pressure at the adjacent vitreous exert both pushing and pulling forces, respectively. The negative pressures in particular may contribute to pathogenesis by applying a tension force as the vitreous pulls away from the posterior pole of the retina, exerting tractional stress on the vitreoretinal adhesions. With great enough magnitude, the retinal vasculature, where vitreoretinal adhesion is greater than tissue lacking vessels, may hemorrhage as a result of



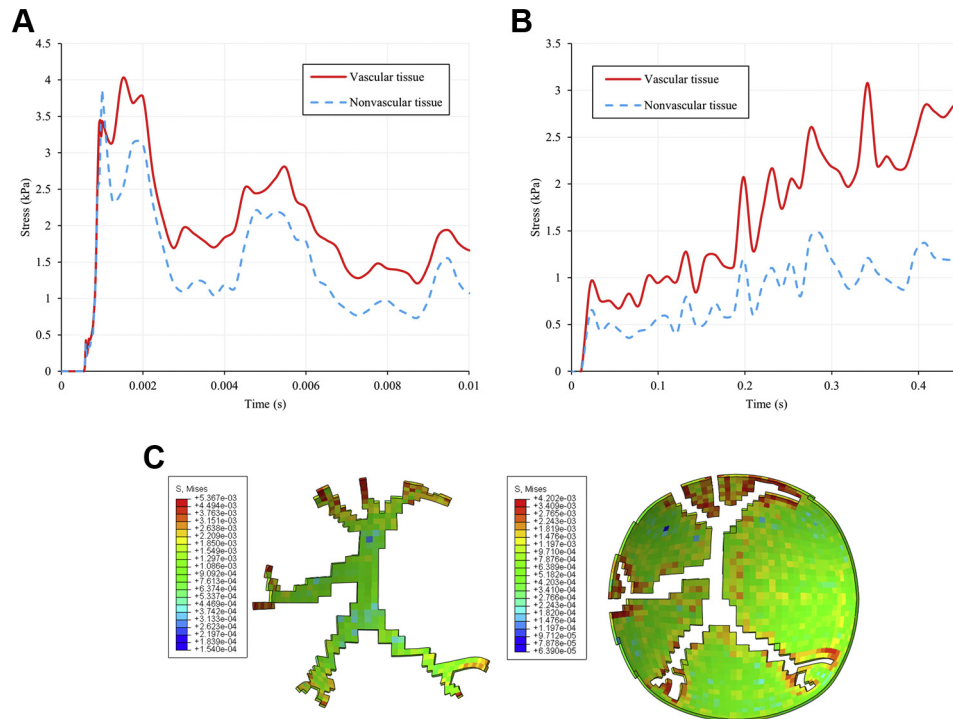


**Figure 6.** Comparison of soccer ball- and abusive head trauma (AHT)-induced stress in the posterior retina. **A**, Line graph showing average soccer ball-induced stress demonstrated by vascular and nonvascular retinal tissue as a function of time. **B**, Line graph showing average AHT-induced stress demonstrated by vascular and nonvascular retinal tissue as a function of time. **C**, Soccer ball-induced stress in the posterior retina visualized as coronal cross-sections of the vascular (left) and nonvascular (right) areas of the posterior retina.

vitreous detachment. Soccer ball-induced stress along the simulated posterior retina was observed to be highest along the vasculature, supporting this hypothesis. The average stress in vascular tissue was observed to peak at roughly 4 kPa, with some individual points at distal vessel bifurcations reaching up to 15.4 kPa, potentially as a result of vessel wall thickness decreasing with successive bifurcations and increased distance from the optic disc. In a prior report studying sheep and primate eyes, the authors determined that the stress required to detach the vitreous from the retina falls within a range of 1 to 5 kPa (Song H, unpublished data, 2021). Thus, stress-induced vitreous detachment may occur after SBOT, potentially accounting for the vitreous hemorrhage observed in 32% of cases.<sup>7</sup>

The form and propagation of the pressure wave may provide insight into the propensity for localization of injury to the posterior retina. The pressure wave was observed to have the highest magnitude in the center as it traveled through the vitreous, likely because of the linear nature of the simulated collision causing most of the energy to continue straight along the anterior–posterior axis, instead of adopting an angled trajectory. Because the posterior pole of the eye is directly in line with the site of impact at the anterior pole, the center of the pressure wave ultimately collided with the posterior retina, leading to higher peak and trough pressures than at peripheral retinal tissue. Other studies have found similar pressure wave oscillation patterns that are most intense at the macula in simulations of other forms of ocular injury, such as blast

loading,<sup>36</sup> likely because blast waves also rapidly exert large amounts of force on the eye. However, the mechanical interactions between the eye and a physical soccer ball or intangible blast wave differ, which results in different velocity profiles and thus variations in retinal injuries.

In addition to retinal hemorrhage, high negative pressure adjacent to the posterior retina may be responsible for other injuries such as retinoschisis, rhegmatogenous retinal detachment, macular hole, and retinal break, which are also observed in SBOT.<sup>7,34</sup> Prior research has shown that the force required to tear or separate the retina from the retinal pigment epithelium to be 9 to 11 kPa,<sup>16,35,37</sup> which may account for the lower incidence of these injuries in comparison with retinal hemorrhage after SBOT. However, it should be noted that obtaining physiologically accurate estimates for these adhesive forces has historically been challenging, and thus may not be representative of in vivo circumstances. Choroidal rupture is another common outcome of blunt trauma injuries such as SBOT, but has relatively low incidence compared with the other aforementioned pathologic characteristics.<sup>7</sup> This may be because of the higher tensile strength of the tissue, most commonly reported as 300 to 330 kPa, far above the stress values observed in this simulation.<sup>14,38</sup> Additionally, the depth of the choroid may protect it from the effects of the rapidly oscillating vitreous pressure. Retinal dialysis has also been observed after SBOT,<sup>5,26</sup> likely because of the dramatic pressure changes of the pressure wave

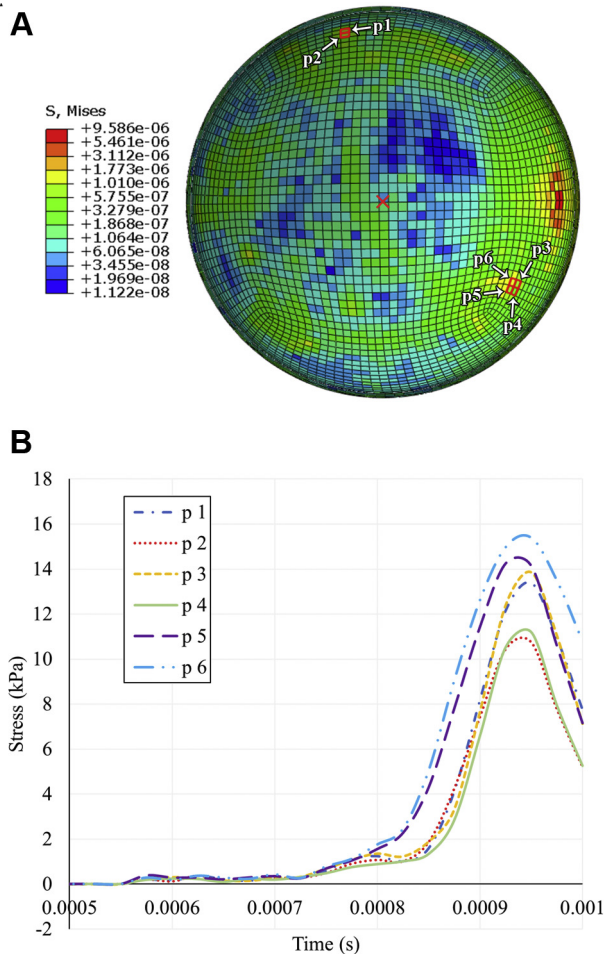


**Figure 7.** Stress distribution at distal branches of the retinal vasculature after impact of a soccer ball at the anterior pole. **A**, Coronal cross-section stress heatmap of the posterior retina. The center of the posterior pole (the macula) is indicated by the red X on the retina heatmap. The 6 selected elements of interest (p1–p6) are outlined in red at points of vessel bifurcation on the retina heatmap. **B**, Line graph showing stress history at the 6 selected elements representing distal vasculature.

affecting anterior tissue after having reflected from the posterior retina.

Examination of the stress experienced in each simulated retinal layer revealed that the subretinal layer showed the highest peak stress after collision, which then decayed over time to values similar to the stress values in the preretinal and intraretinal layers. This initial peak may be the result of the incompressibility of the ocular tissues deep to the subretinal retina, such as the relatively tougher sclera. On initial impact of the soccer ball, the subretinal layer is likely compressed by the pressure wave and experiences a high level of stress because the energy is not readily transferred to the rigid structures deep to it. In comparison, the preretinal and intraretinal layers are also pressed backward by the pressure wave, but are able to disperse energy because of the compressible nature of the retinal tissue deep to these layers, thus resulting in less experienced stress. This trend differs in vascular retinal tissue, wherein the preretinal and intraretinal layers experience slightly more stress than the

subretinal layer. This difference is potentially the result of the vitreoretinal adhesions attached to the preretinal layer being stressed by the tractional force of the pressure wave in the vitreous.

Although this tugging of the vitreoretinal adhesions by the vitreous has historically been considered a likely mechanism for retinal lesions after blunt trauma, a 2010 case reported by Rossi et al<sup>35</sup> described a patient who sustained retinal damage after being shot in the eye by a BB pellet, despite that eye previously having undergone primary pars plana vitrectomy. This case suggests that vitreoretinal traction at adhesions alone cannot account for blunt trauma-related retinal lesions. Another factor at play may be negative pressure within the vitreous leading to a cavitation force that directly pulls the retina anteriorly and stresses adhesions between the layers of the retina and within the retinal pigmented epithelium. This stress throughout the retina may account for the relatively high prevalence of retinal hemorrhage in SBOT.

Although some previous studies reported injury to the posterior retina after SBOT, others have reported concentration of injury to the superior temporal quadrant.<sup>7</sup> The offered explanation for this predilection is that soccer balls are typically kicked upward off the ground and thus strike the eye from below, damaging the superior retina opposite the point of impact. Additionally, the bony orbit and nose provide a degree of protection to the nasal retina on collision. The simulation presented in this study shows extensive pressure oscillations at the posterior pole and thus offers a potential explanation for injuries localized at the posterior retina, but cannot immediately account for superior temporal lesions. However, this may be a limitation of the simulation setup in which the soccer ball approaches the eye from straight ahead with no angle. The authors postulate that had the ball struck the eye from below, the same pressure wave may have been observed in the vitreous, but running linearly along an oblique axis from the point of impact to the superior retina, as opposed to along the anterior–posterior axis. In this situation, the pressure oscillations likely would be greatest at the superior retina, instead of the posterior retina, which would be more consistent with the superior temporal retinal lesions observed in some reports. Further simulations that emulate a variety of angles and conditions would be necessary to confirm this. Overall, the posterior and superior temporal localization of retinal damage observed in SBOT seems to result from the dramatic pressure oscillations in the vitreous, localized depending on the angle at which the ball collides with the eye. For instance, a ball being kicked off the ground may damage the superior retina in a player looking straight ahead because of the eye being struck from below. In contrast, a player looking downward at the ball as it is kicked up may sustain damage to the posterior retina as the ball travels straight into the anterior pole.

Additional future studies to expand on the quantitative results obtained herein include comparing the efficacy of interventions such as protective eyewear. By reducing the transfer of energy from the ball to the eye, eyewear such as safety goggles may attenuate the stress experienced by retinal tissue and may limit the destructive potency of the

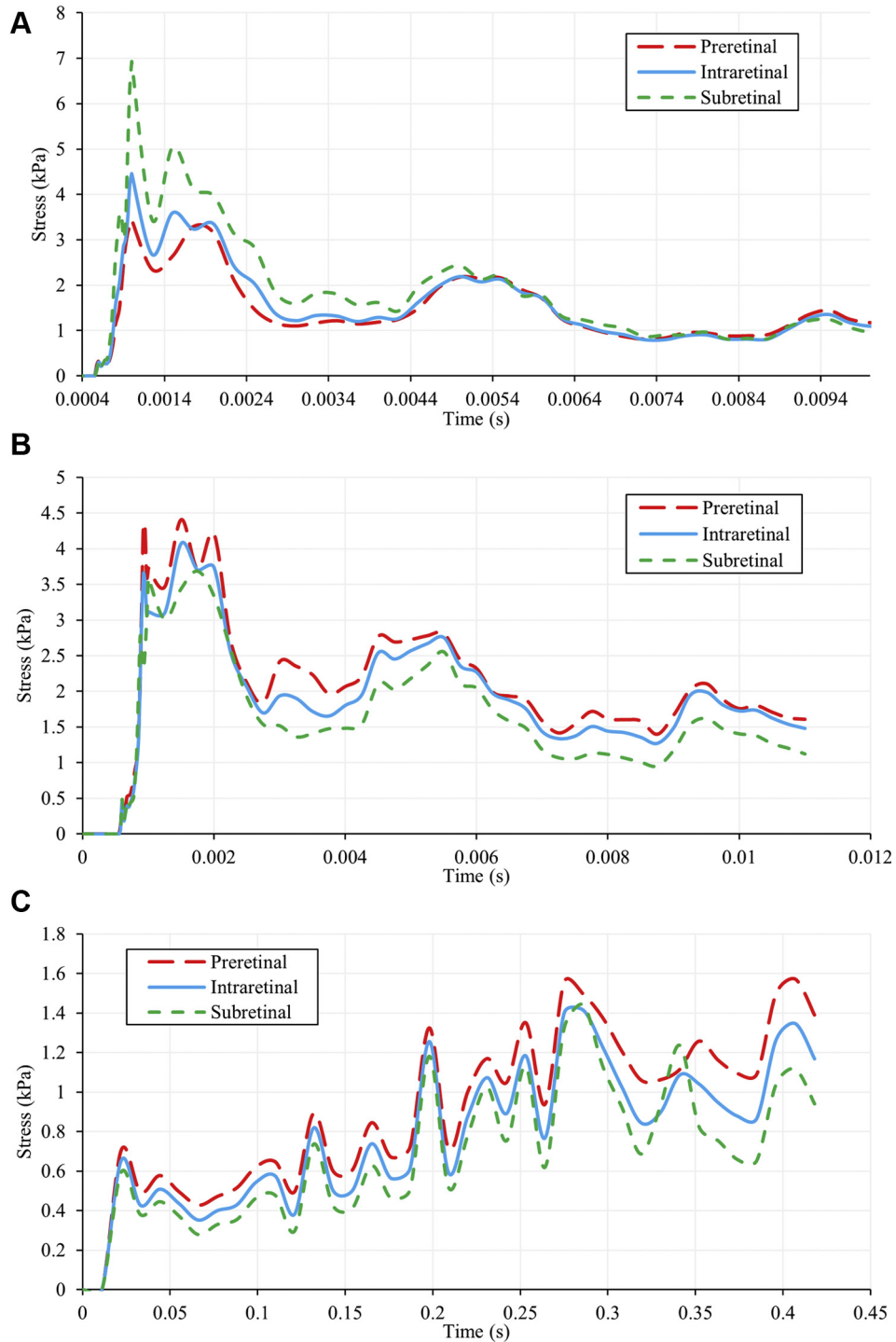


**Figure 8.** Line graphs comparing stress in the preretinal, intraretinal, and subretinal layers in (A) soccer ball ocular trauma (SBOT), (B) SBOT (vascular tissue only), and (C) abusive head trauma.

pressure wave in the vitreous. Lenses of various shapes and materials may be modeled with the eye, then subjected to the trauma scenario used in this simulation to evaluate how stress values and distribution within the eye change in comparison with the findings of this study. Other important factors such as the potential for shattering and bending can

be investigated as well. Further experiments elucidating the biomechanical properties of the eye may also be performed to improve the detail and capabilities of the FE eye model. This would allow for evaluation of other common pathologic features seen after trauma such as commotio retinae and confirmation of existing parameters such as the stress

threshold for choroidal rupture. Such a model could also be applied more broadly to investigate other forms of trauma.

### Soccer Ball Ocular Trauma Compared with Abusive Head Trauma

The authors previously studied the effects of violent shaking of infants to the eye using the same FE simulation. Some differences highlight the various mechanisms by which AHT and SBOT cause injury to the eye, particularly the retina. One such difference is the duration of retinal stress. Stress over time varies more widely in AHT and tends to climb as shaking continues (Fig 8C), in contrast to the peak and decay pattern observed in the current study (Fig 8A, B). As a result, trauma resulting from soccer ball impact may cause vitreous detachment less frequently than AHT, in which a longer duration of trauma potentially leads to tissue fatigue that reduces the force necessary for mechanical tissue failure. This element of tissue fatigue may contribute to the higher rate of retinal hemorrhage seen in AHT compared with SBOT; a 2013 systematic review found that retinal hemorrhage is observed in 78% of patients with AHT, whereas an 8-year observational study recorded retinal hemorrhage in 39% of patients with SBOT.<sup>7,39</sup>

Although stress is concentrated along vasculature in both SBOT and AHT, comparison of the current and previous simulations reveals that the effect is much less pronounced in SBOT. Figure 6 demonstrates that after the initial impact of a soccer ball, the average stress at the vascular retina was roughly 0.5 kPa higher than that of the nonvascular retina. In relative terms, the ratio of stress at the vascular and nonvascular tissues was, at most, approximately 1.8 (calculated at  $t = 3$  ms; 2.0 kPa/1.1 kPa). In AHT, the difference in stress between vascular and nonvascular tissue is initially small, but increases over time as shaking continues. By 341 ms, the stress differential reaches 1.9 kPa, and the relative ratio is 2.6 (calculated at  $t = 341$  ms; 3.1 kPa/1.2 kPa).

This difference in distribution of retinal stress between SBOT and AHT injuries can likely be attributed to the differing underlying accelerative forces behind the two injuries. A collision of a soccer ball with the eye is similar to heading a soccer ball, with the main difference lying in the point of contact of the head and ball. Proper heading of a soccer ball produces almost entirely linear acceleration of the head; therefore, SBOT likely imparts force such that the eye experiences mostly linear acceleration as well.<sup>40</sup> In contrast, AHT generates significant amounts of both linear and angular acceleration.<sup>41</sup>

Linear acceleration imparts compressive and tractional force onto the retina through a pressure wave that travels linearly from the point of impact, as previously discussed. Linear acceleration originating from a soccer ball collision in particular may impart an extraordinarily potent tractional force because soccer balls have been observed to deform on contact with the face and exert a suction effect on the orbit as they bounce off after collision.<sup>13</sup> In comparison, angular acceleration produces a shearing force between ocular surfaces such as the vitreous, retinal vessels, and the underlying retina (Song H, unpublished data, 2021), which

may account for the greater stress differential between vasculature and adjacent tissue observed in AHT. Linear acceleration is present in both SBOT and AHT, whereas angular acceleration is present only in AHT, providing a possible explanation for the comparatively lower stress differential between vessels and surrounding tissue in SBOT.

This difference in forces at play during injury may also account for the varying localizations of injury between AHT and SBOT. Rapid shaking of the head in all directions during AHT induces angular acceleration and deceleration of the eye in all directions. The entirety of the vitreous body is thus subjected to these forces and consequently exerts shearing forces throughout the retina. This likely accounts for the diffuse, nonlocalized distribution of injury that often results from AHT, differing from the more localized pattern of retinal lesions seen in SBOT.<sup>9</sup>

This work used an FE simulation to investigate the underlying pathophysiologic features and biomechanics of ocular and retinal pathologic features resulting from SBOT. Given the worldwide popularity of soccer, studying the associated injuries will provide clinicians a greater understanding of a relatively common sports injury, especially those that work with a pediatric patient population. Additionally, modeling and quantifying the underlying biomechanical events will allow for effective development of protective eyewear designed to mitigate the mechanisms of injury. The model revealed that anterior segment injuries such as hyphema and angle recession may be attributed to high pressure and stress resulting from direct contact and transfer of energy from the soccer ball. Posterior segment injuries, particularly retinal lesions like vitreous and retinal hemorrhage and retinal detachment, may arise from the propagation of a pressure wave in the vitreous that exerts both compressive and tractional forces on the retina and vitreoretinal adhesions. These distinct mechanisms give rise to a set of injuries and incidences characteristic of SBOT. This set of injuries differs from those seen in other settings such as AHT, which has its own classical presentation because of differing underlying pathophysiologic features. This work demonstrated how transient, linear force generated by a soccer ball can produce posteriorly localized retinal lesions, whereas the authors' previous FE simulation study provided insight into how the repetitive, multidirectional angular forces at work in AHT result in a diffuse, multilayer pattern of retinal hemorrhage. Better understanding of how the biomechanics underlying different ocular injuries result in distinct patterns of pathologic features through works such as these will assist clinicians in discerning the history of presenting injuries. This will not only prove beneficial in guiding treatment and prevention, but may also have important legal implications in cases of suspected abuse or other foul play.

### Acknowledgments

The authors thank Dr Don Minckler for providing valuable insight, guidance, and discussion during the preparation of this work and Dr Angele Nalbandian for assisting with the editing of this article.

## Footnotes and Disclosures

Originally received: August 18, 2021.

Final revision: January 11, 2022.

Accepted: February 14, 2022.

Available online: February 20, 2022. Manuscript no. XOPS-D-21-00146.

<sup>1</sup> Creighton University School of Medicine, Omaha, Nebraska.

<sup>2</sup> Florida Institute of Technology, Department of Biomedical and Chemical Engineering & Department of Mechanical Engineering, Melbourne, Florida.

<sup>3</sup> Gavin Herbert Eye Institute, University of California at Irvine, Department of Ophthalmology and Visual Sciences, Irvine, California.

Disclosure(s):

All authors have completed and submitted the ICMJE disclosures form.

The author(s) have no proprietary or commercial interest in any materials discussed in this article.

Supported by Research to Prevent Blindness, Inc., New York, New York (unrestricted grant to the Gavin Herbert Eye Institute at the University of California, Irvine).

HUMAN SUBJECTS: No human subjects were included in this study. The Institutional Review Board approved the study. The requirement for informed consent was waived because of the retrospective nature of the

study. Individual patient-level consent was not required for this study. All research adhered to the tenets of the Declaration of Helsinki.

No animal subjects were included in this study.

Author Contributions:

Conception and design: Lam, Dong, Shokrollahi, Gu, Suh

Analysis and interpretation: Lam, Dong, Shokrollahi, Gu, Suh

Data collection: Dong, Shokrollahi, Gu

Obtained funding: N/A

Overall responsibility: Lam, Dong

Abbreviations and Acronyms:

**AHT** = abusive head trauma; **FE** = finite element; **SBOT** = soccer ball ocular trauma.

Keywords:

Abusive head trauma, Blunt trauma, Computer simulation, Retinal hemorrhage, Sports injury.

Correspondence:

Matthew R. Lam, Creighton University School of Medicine, 2500 California Plaza, Omaha, NE 68178. E-mail: [matthewlam@creighton.edu](mailto:matthewlam@creighton.edu).

## References

- Goldstein MH, Wee D. Sports injuries: an ounce of prevention and a pound of cure. *Eye Contact Lens*. 2011;37(3):160–163.
- Napier SM, Baker RS, Sanford DG, Easterbrook M. Eye injuries in athletics and recreation. *Surv Ophthalmol*. 1996;41(3):229–244.
- Haring RS, Sheffield ID, Canner JK, Schneider EB. Epidemiology of sports-related eye injuries in the United States. *JAMA Ophthalmol*. 2016;134(12):1382–1390.
- Miller KN, Collins CL, Chounthirath T, Smith GA. Pediatric sports- and recreation-related eye injuries treated in US emergency departments. *Pediatrics*. 2018;141(2):e20173083.
- Mishra A, Verma AK. Sports related ocular injuries. *Med J Armed Forces India*. 2012;68(3):260–266.
- Arias E, Tejada-Vera B, Ahmad F. Provisional life expectancy estimates for January through June, 2020. Vital Statistics Rapid Release, report no. 10. Hyattsville, MD: National Center for Health Statistics, Division of Vital Statistics; 2021. <https://doi.org/10.15620/cdc:100392>. Accessed July 14, 2021.
- Capao Filipe JA, Fernandes VL, Barros H, et al. Soccer-related ocular injuries. *Arch Ophthalmol*. 2003;121(5):687–694.
- Giannotti M, Al-Sahab B, McFaull S, Tamim H. Epidemiology of acute head injuries in Canadian children and youth soccer players. *Injury*. 2010;41(9):907–912.
- Suh DW, Song HH, Mozafari H, Thoreson WB. Determining the tractional forces on vitreoretinal interface using a computer simulation model in abusive head trauma. *Am J Ophthalmol*. 2021;223:396–404.
- Bekerman I, Gottlieb P, Vaiman M. Variations in eyeball diameters of the healthy adults. *J Ophthalmol*. 2014;2014:503645.
- Creveling CJ, Colter J, Coats B. Changes in vitreoretinal adhesion with age and region in human and sheep eyes. *Front Bioeng Biotechnol*. 2018;6:153.
- Tsui I, Pan CK, Rahimy E, Schwartz SD. Ocriplasmin for vitreoretinal diseases. *J Biomed Biotechnol*. 2012;2012:354979.
- Vinger PF, Capao Filipe JA. The mechanism and prevention of soccer eye injuries. *Br J Ophthalmol*. 2004;88(2):167–168.
- Friberg TR, Lace JW. A comparison of the elastic properties of human choroid and sclera. *Exp Eye Res*. 1988;47(3):429–436.
- Bisplinghoff JA, McNally C, Duma SM. High-rate internal pressurization of human eyes to predict globe rupture. *Arch Ophthalmol*. 2009;127(4):520–523.
- Wollensak G, Spoerl E. Biomechanical characteristics of retina. *Retina*. 2004;24(6):967–970.
- Bassnett S. Zinn's zonule. *Prog Retin Eye Res*. 2020;100902.
- Delamere NA. Ciliary body and ciliary epithelium. *Adv Organ Biol*. 2005;10:127–148.
- Feng MT, Belin MW, Ambrosio Jr R, et al. Anterior chamber depth in normal subjects by rotating Scheimpflug imaging. *Saudi J Ophthalmol*. 2011;25(3):255–259.
- Praveen MR, Vasavada AR, Shah SK, et al. Lens thickness of Indian eyes: impact of isolated lens opacity, age, axial length, and influence on anterior chamber depth. *Eye (Lond)*. 2009;23(7):1542–1548.
- Canavan YM, Archer DB. Anterior segment consequences of blunt ocular injury. *Br J Ophthalmol*. 1982;66(9):549–555.
- Gragg J, Blair K, Baker MB. <https://www.ncbi.nlm.nih.gov/books/NBK507802>. *HypHEMA*. *StatPearls*. 2020. Accessed February 21, 2021.
- Blanton FM. Anterior chamber angle recession and secondary glaucoma. A study of the aftereffects of traumatic hyphemas. *Arch Ophthalmol*. 1964;72:39–43.
- Razeghinejad R, Lin MM, Lee D, et al. Pathophysiology and management of glaucoma and ocular hypertension related to trauma. *Surv Ophthalmol*. 2020;65(5):530–547.
- Mahabadi N, Kim J, Edens MA. Iritis. *StatPearls*; 2021. <https://www.ncbi.nlm.nih.gov/books/NBK430909>, March 22, 2021.
- Kaufman JH, Tolpin DW. Glaucoma after traumatic angle recession. A ten-year prospective study. *Am J Ophthalmol*. 1974;78(4):648–654.

27. Phelps CD, Watzke RC. Hemolytic glaucoma. *Am J Ophthalmol*. 1975;80(4):690–695.
28. Bhardwaj V, Rajeshbhai GP. Axial length, anterior chamber depth—a study in different age groups and refractive errors. *J Clin Diagn Res*. 2013;7(10):2211–2212.
29. Kennedy EA, Voorhies KD, Herring IP, et al. Prediction of severe eye injuries in automobile accidents: static and dynamic rupture pressure of the eye. *Annu Proc Assoc Adv Automot Med*. 2004;48:165–179.
30. Kumar K, Figurasin R, Kumar S, Waseem M. An uncommon meridional globe rupture due to blunt eye trauma. *Case Rep Emerg Med*. 2018;2018:1808509.
31. Moore KL, Dalley AF, Agur AMR. *Clinically Oriented Anatomy*. 8th ed. Philadelphia: Wolters Kluwer; 2018.
32. Turvey TA, Golden BA. Orbital anatomy for the surgeon. *Oral Maxillofac Surg Clin North Am*. 2012;24(4):525–536.
33. Liu X, Wang L, Ji J, Fan Y. The protective effect of the eyelid on ocular injuries in blunt trauma. In: Jaffray DA, ed. *IFMBE Proceedings*. Vol. 51. *World Congress on Medical Physics and Biomedical Engineering, June 7–12, 2015*. Switzerland: Springer International Publishing; 2015:338–341.
34. Horn EP, McDonald HR, Johnson RN, et al. Soccer ball-related retinal injuries: a report of 13 cases. *Retina*. 2000;20(6):604–609.
35. Rossi T, Boccassini B, Esposito L, et al. The pathogenesis of retinal damage in blunt eye trauma: finite element modeling. *Invest Ophthalmol Vis Sci*. 2011;52(7):3994–4002.
36. Esposito L, Clemente C, Bonora N, Rossi T. Modelling human eye under blast loading. *Comput Methods Biomech Biomed Engin*. 2015;18(2):107–115.
37. Wollensak G, Spoerl E, Grosse G, Wirbelauer C. Biomechanical significance of the human internal limiting lamina. *Retina*. 2006;26(8):965–968.
38. Djigo AD, Berube J, Landreville S, Proulx S. Characterization of a tissue-engineered choroid. *Acta Biomater*. 2019;84:305–316.
39. Maguire SA, Watts PO, Shaw AD, et al. Retinal haemorrhages and related findings in abusive and non-abusive head trauma: a systematic review. *Eye (Lond)*. 2013;27(1):28–36.
40. Reed WF, Feldman KW, Weiss AH, Tencer AF. Does soccer ball heading cause retinal bleeding? *Arch Pediatr Adolesc Med*. 2002;156(4):337–340.
41. Yamazaki J, Yoshida M, Mizunuma H. Experimental analyses of the retinal and subretinal haemorrhages accompanied by shaken baby syndrome/abusive head trauma using a dummy doll. *Injury*. 2014;45(8):1196–1206.